Scientia Iranica, Vol. 15, No. 1, pp 131–143

SCIENTIA
IRANICA

Research Note

Maximum Dynamic Load Carrying Capacity of a 6UPS-Stewart Platform Manipulator

M.H. Korayem* **and M. Shokri**[1]

In this paper, a computational method for obtaining the maximum Dynamic Load Carrying Capacity (DLCC) for the 6-UPS Stewart platform manipulator is developed. In this paper, the manipulator is assumed to be non-rigid and the joint actuator torque capacity and accuracy of motion are considered major limiting factors in determining the maximum payload. The maximum dynamic payload carrying capacity of the manipulator is established, while the dynamic model of a typical hydraulic actuator system is used in the joint actuator force capacity for a given trajectory. The flexibility of the manipulator is assumed to be eventuated from the manipulator's joints flexibility. According to the high complexity of the dynamic equations system of the flexible joints parallel manipulators, the effects of the flexibility of the prismatic joints are considered in a static situation to show the considerable effects of the joint's flexibility on the motion accuracy of the 6UPS-Stewart platform. This method can be used for determining the maximum dynamic payload, which acts as an end-effector for the mechanical design of the manipulator and the optimized selection of the actuator, such as machine tools, based on the hexapod mechanism.

INTRODUCTION

The Dynamic Load Carrying Capacity (DLCC) of a robot manipulator is a method of presenting the relationship between dynamic performance and actuator torque capacity and is defined as the maximum payload that the manipulator can repeatedly lift in its fully extended configuration, while the dynamics of both the load and the robot manipulator itself must be taken into account. For the rigid manipulators, the major limiting factor in determining maximum load is the joint actuator capacity. For flexible joint manipulators, a flexible deformation constraint should also be considered for the predefined trajectory, since the flexible deformation of joints has an effect on the precision of the dynamic trajectory of the end-effector.

There are some applications of a parallel robot manipulator that determine the maximum DLCC of the manipulator. For a given trajectory, it is very important to select the optimized joint actuator capacity and vice-versa. Using machine tools, based on hexapod manipulators, is one application of a parallel manipulator where the determination of the DLCC is critical in the mechanical design of the machine and the manipulator. In this paper, the DLCC of a 6UPS-Stewart platform and a computational approach for determining its maximum load is developed. The Stewart platform is an example of a parallel connection robot manipulator and its structure is obtained from a generalization of the mechanism originally proposed by Stewart as a flight simulator. The position and orientation of the moving platform are controlled by the lengths of the six legs actuated by six prismatic joints. Each leg is connected to the base by a 2-DOF universal joint and connected to the moving platform by a 3-DOF spherical joint [1,2].

The DLCC problem of a robot manipulator was studied about two decades ago. Important research in this field was done by Wang and Ravani [3,4]. They studied the problem associated with the load-carrying capacity of mechanical manipulators and found that the problem of synthesizing a point-to-point dynamic robot motion with an optimum load-carrying capacity can be formulated as a trajectory optimization problem. Other considerable research was done by Bowling and Khatib [5,6]. They introduced the Dynamic Capability Equations (DCE) as a new tool for analyzing robotic manipulator performance. These equations

*. *Corresponding Author, Department of Mechanical Engineering, Iran University of Science and Technology, Tehran, I.R. Iran.*

1. *Department of Mechanical Engineering, Iran University of Science and Technology, Tehran, I.R. Iran.*

describe the magnitudes of translational and rotational acceleration and force guaranteed to be achievable in every direction, from a particular configuration, given the limitations on the manipulator's motor torques. There are some works concerning DLCC problems in an open-chained manipulator, in which flexible deformation and joint actuator capacity are considered as a limiting factor [7-9].

There has been considerable research undertaken on the DLCC of parallel manipulators. For example, Yong Sheng Zhao and his coworkers introduced a novel unified method for computing the dynamic load carrying capacity of multiple cooperating robotic manipulators [10]. Han S. Kim and J. Choi introduced an analytical method to evaluate the forward and inverse force transmission capability of fully parallel manipulators [11]. Merlet considered a classical Gaugh platform with extensible legs, which is submitted to a given load and the values of the articular forces were determined when the platform was translated into a given 3D workspace. In this algorithm, the orientation of the platform is assumed to be constant [12]. Nokleby and his coworker introduced a methodology of using a scaling factor to determine the force capability of non-redundant and redundant-actuated parallel manipulators [13].

While a large amount of research has been concentrated on the modeling, analysis and related topics of Stewart platforms, which have been published in the literature, there has been little research concerning the DLCC of parallel manipulators, including the Stewart platform based manipulators. In this paper, a computational approach for obtaining the maximum dynamic load carrying capacity for a 6-DOF parallel manipulator, based on Stewart platforms and called a 6-UPS Stewart platform manipulator, is presented. In this paper, the manipulator is assumed to be a non-rigid manipulator and the joint actuator torque capacity and accuracy of motion are considered as the major limiting factors in determining the maximum payload. The maximum dynamic load carrying capacity of a manipulator is established while the dynamic model of a typical hydraulic actuator system is used in the joint actuator force capacity for a given trajectory. The flexibility of the prismatic joints is considered, in order to model and formulize the motion accuracy constraint. Due to the high complexity of the dynamic equations system of flexible joints in a 6UPS-Stewart platform, the flexibility effects of the prismatic joints are only considered in a static situation, in order to show the considerable effects of the joint's deflection on the motion accuracy of the 6UPS-Stewart platform. This method can be used for determining the maximum dynamic payload, which acts on the end-effector of the manipulator, for the mechanical design of the manipulator and the optimized selection of the actuator, such as machine tools, based on a hexapod mechanism.

In this paper, first, a geometrical model of a 6UPS-Stewart platform is considered and its kinematics are established, based on this model. The dynamics of a 6UPS-Stewart platform are established by using a virtual work principle. Secondly, the DLCC of a 6UPS-Stewart platform is formulated and actuator capacity and accuracy constraints are imposed on the developed DLCC model to determine the maximum load for a given trajectory. A computational algorithm is developed to determine the maximum load of a 6UPS-Stewart platform for a given trajectory, based on the established DLCC model. Finally, the developed algorithm is implemented using mathematics software and its performance is tested by several given trajectories and the results are simulated by using Working Model software.

KINEMATICS AND DYNAMICS MODEL OF THE 6UPS-STEWART PLATFORM MANIPULATOR

The principle of virtual work or the d'Alembert's principle is used for the dynamic analysis of a 6UPS-Stewart platform. In this model, dynamic and gravity forces at the joints are considered. Further, it is assumed that no rotation of any leg about the longitudinal axis of the leg is allowed.

For the kinematics and dynamic analysis, a coordinate frame, $A(x, y, z)$, is attached to the fixed base and another coordinate frame, $B(u, v, w)$, is attached to the moving platform. The $x - y$ plane contains the universal joints, A_i, and the $u - v$ plane contains the ball joints, B_i, for $i = 1 \cdots 6$. The origin of the moving frame, B, is located at the center of the moving platform and the origin of the fixed frame is located at the center of the fixed base. Each of the six limbs is denoted by a vector, S_i. A vector model of a 6-UPS Stewart platform is shown in Figure 1.

A new coordinate frame, $A_i(x_i,\ y_i$ and $z_i)$, is defined for ith limb with the origin located at A_i, as called a joint frame (Figure 1). This frame presents the orientation of each limb relative to the base frame. The unit vector, k_i, of ith joint frame is defined along the leg axis, the unit vector, j_i, along the rotation axis of the universal joint and the unit vector, i_i, perpendicular to k_i and j_i, according to the right hand rule. The length and unit vector of the ith leg is defined as follows:

$$d_i = |S_i| \rightarrow s_i = \frac{S_i}{d_i}. \tag{1}$$

Since each leg of a 6UPS-Stewart platform is connected to a fixed plate by a universal joint, there is no rotation about the longitudinal axis of the leg and the orientation of the leg can be described by two Euler

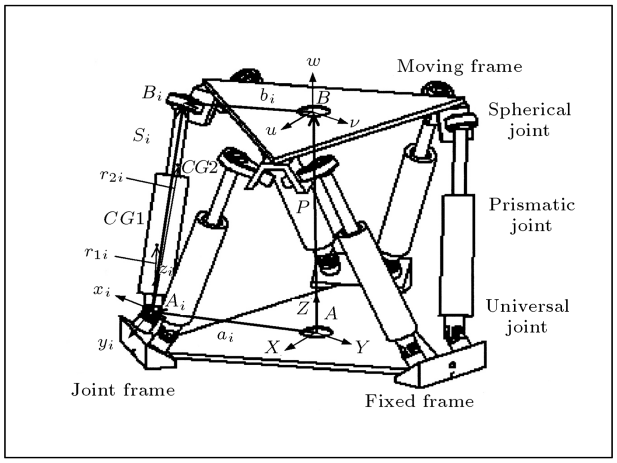

Figure 1. Kinematics configuration and vector model of 6UPS-Stewart platform.

angles, namely, a rotation of φ_i about the z_i-axis, resulting in a (x_i', y_i', z_i') system, followed by another rotation of θ_i about the rotated y_i'-axis. Therefore, the transformation relating the joint frame to the fixed (base) frame can be defined as $R_{\varphi i}.R_{\theta i}$.

By defining the Cartesian coordinate vector, $[x\ y\ z\ \varphi\ \theta\ \psi]^T$, where $[x\ y\ z]^T$ is the position vector and $[\varphi\ \theta\ \psi]^T$ is the orientation vector of the moving platform's mass center, the orientation of the moving platform can be presented by three Euler angles. As shown in Figure 1, the platform connection point, B_i, can be transformed to the base frame as follows:

$$S_i = P + R_{AB} b_{iB} - a_i, \qquad (i = 1, \cdots, 6). \tag{2}$$

This equation is the inverse kinematics equation for the Stewart platform. In this approach, each prismatic joint is modeled as two parts: The lower part (cylinder) and the upper part (piston) and the position vector of the mass center of the lower and upper part of the ith prismatic joint (CG_1 and CG_2 in Figure 1) are r_{1i} and r_{2i}, which are presented as relative to the base frame. The mass and moment of inertia of the lower and upper part of the ith prismatic joint are $(m_{1i},\ I_{1i})$ and $(m_{2i},\ I_{2i})$.

The principle of the virtual work for a 6UPS-Stewart platform can be stated as:

$$\delta q^T \tau + \delta x_p^T F_p + \sum_{i=1}^{6} \delta x_i^T F_i = 0, \tag{3}$$

where τ is the vector of an actuated joint torques/forces, F_p is a six-dimensional wrench, including the sum of the applied and inertia wrenches about the center of mass of the moving platform, F_i is a six-dimensional wrench, including the sum of the applied and inertia wrenches about the center of mass of the ith link and δq, δx_p and δx_i are the virtual displacement of the actuated joint, platform and ith link. The virtual displacement of the actuated joint is related to the virtual displacement of the moving platform, by the manipulator Jacobean matrix, J_p, and the virtual displacement of the ith link can be related to the virtual displacement of the moving platform, by a link Jacobean matrix, J_i. The manipulator and link Jacobean matrices can be determined by using the vector loop equation, which is written based on Equation 2. For a 6UPS-Stewart platform, the equation of motion can be written as follows:

$$J_p^T \tau + F_p + \sum_{i=1}^{6} (J_{1iAi}^T F_{1iAi} + J_{2iAi}^T F_{2iAi}) = 0, \tag{4}$$

where J_{1Aii} and J_{2Aii} are the link Jacobean matrices and F_{1Aii} and F_{2Aii} are the wrenches, including the sum of the applied and inertia forces of the lower and upper part of the ith link, relative to the joint frame which can be expressed as follows:

$$F_{kAii} = \begin{pmatrix} m_{ki} g_{Ai} - m_{ki} a_{kiAi} \\ -I_{kiAi} \alpha_{kiAi} - \omega_{kiAi} \times (I_{kiAi} \omega_{kiAi}) \end{pmatrix},$$

$$k = 1, 2. \tag{5}$$

FORMULATION OF DYNAMIC LOAD CARRYING CAPACITY FOR A PRESCRIBED TRAJECTORY

By supposing that the load is located on a moving platform, rigidly, the moving platform and load can be considered as a rigid body. So, the load effect on the dynamic behavior of the manipulator can be accounted for by using the compound body, which is the equivalent of the moving platform and load. Therefore, an equivalent mass, (m_C), mass center, (C_C), and moment of inertia, (I_C), relative to a moving coordinate system can be defined for a compound body as follows:

$$m_c = m_p + m_L, \tag{6}$$

$$C_c = \frac{m_p C_p + m_L C_L}{m_p + m_L}, \tag{7}$$

$$I_c = I_p + m_p [C_p^*]^T [C_p^*] + I_L + m_L [C_L^*]^T [C_L^*], \tag{8}$$

where m_P and m_L are the mass of the moving platform and load, respectively; C_P and C_L are the position vector of the moving platform mass center and the position vector of the load mass center, relative to the moving coordinate system, respectively, and I_P is the moving platform about itself mass center, and I_L is the load moment of inertia relative to the moving coordinate system. C_P^* and C_L^* can be defined as $C_P^* = C_C - C_P$ and $C_L^* = C_C - C_L$. The position,

velocity and acceleration vectors of a compound body, relative to a fixed coordinate system, can be calculated, based on the position, velocity and acceleration vector loop of each leg. According to the equation of motion of the moving platform (Equation 5) the load effect on the dynamic behavior of the manipulator can be presented as follows:

$$J_p^T \tau + F_c + \sum_{i=1}^{6} (J_{1iAi}^T F_{1iAi} + J_{2iAi}^T F_{2iAi}) = 0, \qquad (9)$$

where F_c is a wrench, including the sum of the applied and inertia forces about the equivalent mass center of the load and platform, defined as:

$$F_c = \begin{pmatrix} m_c g - m_c(a_p + \alpha_p \times C_c + \omega_p \times (\omega_p \times C_c)) \\ -I_c \alpha_p - \omega_p \times (I_c \omega_p) \end{pmatrix}, \qquad (10)$$

where ω_p, a_p and α_p are angular velocity, linear and angular acceleration vectors of the mass center, relative to the fixed coordinate system.

Formulation of the Joint Actuator Constraint

In a 6UPS-Stewart platform, the joint actuator is a hydraulic/pneumatic linear actuator. The torque constraint of a hydraulic/pneumatic linear actuator can be formulated, based on the torque-speed characteristics. There is much research into determination of the dynamic model of hydraulic/pneumatic linear actuators. The analysis of a typical hydraulic servo-system is well documented in [14]. A power curve for power saving circuits can be plotted, so that any two force-speed coordinates intersecting on the curve represent the input power for which the curve is designed. The power of a hydraulic actuator system is:

$$P_H = \eta P_s . q_{\max}, \qquad (11)$$

in which P_h is hydraulic power, P_s is supply pressure, q is flow rate and η is efficiency coefficient, which is determined, based on the internal friction of the actuator and the internal leakage of the valve and actuator. The maximum flow rate of a hydraulic actuation system can be determined, based on the maximum operating velocity of the actuator. By supposing that the maximum desired velocity for the positive and negative stroke is $V_{\max}$, the maximum flow rate in the positive and negative stroke can be expressed as:

$$q_{\max}^{+} = A^{+} . V_{\max}, \qquad (12a)$$

$$q_{\max}^{-} = A^{-} . V_{\max}, \qquad (12b)$$

where A^+ and A^- are the effective piston area with a positive and negative stroke. The hydraulic power of a given actuation system is spent to overcome the load and internal friction forces. Thus, the hydraulic power is converted to mechanical power. The produced mechanical power generates a total force, which is acting to the system and velocity of the piston. This means that an actuator with a fast approach speed and an output force would require an input power, P, and when switched to a slow work speed under the same power consumption, would produce a larger force. The relation between the generated force and the working velocity of the hydraulic system can be shown as a power curve (force-speed curve), which is shown in Figure 2 for a typical hydraulic system, where V_1 and V_2 are two different working speeds and F_1 and F_2 are the available forces of the actuator, respectively. By supposing the internal friction forces to be 15% of the total force acting on the system, the maximum available force of a given hydraulic actuator system, with positive and negative strokes, can be written as:

$$F_{a\,\max}^{+} = 0.85 \frac{P_s . q_{\max}^{+}}{\dot{x}}, \qquad (13a)$$

$$F_{a\,\max}^{-} = 0.85 \frac{P_s . q_{\max}^{-}}{\dot{x}}, \qquad (13b)$$

where $\dot{x}$ is the piston velocity at each point of the motion path. For hydraulic actuator force capability analysis, q is determined, based on the piston velocity, which is given for the prescribed task. For a given velocity of the piston, the flow rate can be written as a product of the effective piston area and the piston velocity. If F_a^+ and F_a^- are the upper and lower bounds of the available actuator force at each point of the trajectory, F_{nai} and F_{pai} are the ith actuated joint force for a no-load condition and by adding the moving platform mass as a sample mass, respectively, the upper and lower bound of actuator force can be determined as follows:

$$(F^+)_i = (F_a^+)_i - F_{ai}, \qquad (14a)$$

$$(F^-)_i = (F_a^-)_i - F_{ai}. \qquad (14b)$$

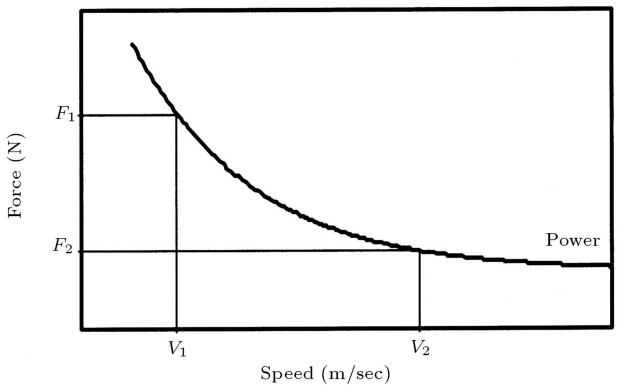

Figure 2. Force-speed curve of typical hydraulic system.

Therefore, the maximum allowable actuator force of the ith actuated joint is:

$$F_i = \{(F^+)_i, (F^-)_i\}. \tag{15}$$

Now, a load coefficient ($C_{i-\text{Torque}}$) complying with the actuator force constraint for each point of the trajectory can be defined as:

$$C_{i-\text{Torque}} = \min\left\{\frac{F_i}{F_{pai} - F_{nai}} \rightarrow i = 1, 2, \cdots, n\right\}. \tag{16}$$

The load coefficient, as to the actuator torque capacity constraint ($C_{\text{Load}-\text{Torque}}$) of the trajectory, can be selected as the minimum value of $C_{i-\text{Torque}}$.

Formulation of the Accuracy Constraint

Deflection at the end-effector could be attributed to both static and dynamic factors, such as, joint clearance, manipulator and load inertia. The DLCC of flexible manipulators is motion dependent, since these factors are configuration or motion dependent. If $w \in R^6$ is considered as the coordinate of a point on the desired path of motion and $w' \in R^6$ as the coordinate of a point on the actual path of motion, the deflection of the end-effector at this point can be expressed as follows:

$$\Delta w = w' - w.$$

The small displacement of the end-effector can be related to the small displacement of the actuated joint as $\Delta w = J\Delta q$, where J is the manipulator Jacobean matrix and Δq is the flexible deformation of the actuated joint and is expressed as $\Delta q = q' - q$. q is the desired displacement and q' is the actual displacement of the actuator. The flexibility of each actuated joint can be described by a spring constant, K, and expressed as $\tau = K\Delta q$, where τ is the torque of the actuated joint. Thus, the deflection of the end-effector can be related to the actuator torque in a static condition as follows:

$$\Delta w = JK^{-1}\tau. \tag{17}$$

In this paper, the prismatic joint of each limb is assumed flexible and other joints are assumed to be rigid for simplicity. The flexibility of a flexible joint can be modeled by a linear spring with spring constant K. Closed kinematics chains with flexibility introduce constraint equations systems that are very complex and are difficult to solve, due to the complex relationships of the equations and the coupling between the algebraic and differential equations. Accordingly, in this paper, Equation 17 is used for calculation of the deflection of the end-effector by imposing an accuracy constraint to show the great effect of joint flexibility on the load factor of the 6UPS-Stewart platform. In this approach, deflection of the end-effector is calculated in a static condition for each point of the trajectory. Actuator forces, which are calculated by dynamic models, are used for deflection determination to provide closer results to the dynamic condition.

The translational deflection of the end-effector at each point of the path can be expressed by a constant value, which introduces an allowable radius of sphere of translational deflection for modeling the accuracy of the motion constraint in DLCC determination. An allowable radius of sphere of translational deflection can be expressed as:

$$\Delta P = \sqrt{\Delta w_1^2 + \Delta w_2^2 + \Delta w_3^2}, \tag{18}$$

where Δw_1, Δw_2 and Δw_3 are allowable deflection in x, y and z directions, respectively. The orientation deflection of the end-effector can be expressed by three values, which introduce allowable deflection for each orientation deflection, such as $-\alpha \leq \Delta w_4 \leq \alpha$, $-\beta \leq \Delta w_5 \leq \beta$ and $-\gamma \leq \Delta w_6 \leq \gamma$.

For DLCC determination, by imposing an accuracy of motion constraint, first, the deflection vector of the end-effector for a no-load condition, Δw_n, and then, by adding the end-effector mass, Δw_e is calculated for each point of the path of motion. The additional mass at the end-effector changes both the magnitude and direction of the deflection. But, as long as the magnitude of the deflection is less than, or equal to, an allowable value, the robot is considered to remain capable of executing the given trajectory [7]. In other words, only the magnitude of the deflection needs to be considered in this context. In the following, by adding the end-effector mass ($\Delta w_{ai} = [\Delta P_{axi}\ \Delta P_{ayi}\ \Delta P_{azi}\ \Delta w_{a1i}\ \Delta w_{a2i}\ \Delta w_{a3i}]^T$) the available deflection vector is calculated at each point of the path of motion as follows:

$$\Delta P_{ai} = \delta^P - \Delta P_{ei}, \tag{19a}$$

$$\Delta w_{a1i} = \delta_1^r - \Delta w_{1ei}, \tag{19b}$$

$$\Delta w_{a2i} = \delta_2^r - \Delta w_{2ei}, \tag{19c}$$

$$\Delta w_{a3i} = \delta_3^r - \Delta w_{3ei}, \tag{19d}$$

where ΔP_{ei} is the translational deflection vector in x, y and z directions, Δw_{1ei}, Δw_{2ei} and Δw_{3ei} are orientation deflections, by adding the end-effector mass, respectively, δ^P is the allowable radius of the allowanced sphere of the translation deflection and δ_1^r, δ_2^r and δ_3^r are the allowable values for φ, θ and ψ directions of orientation deflection, respectively. Therefore, the load coefficient of translation deflection and orientation

deflections ($C_{ki} \rightarrow k = 1, 2, 3, 4$), respectively, can be expressed as:

$$C_{1i} = \frac{\Delta P_{ai}}{\Delta P_{ei} - \Delta P_{ni}}, \tag{20a}$$

$$C_{2i} = \frac{\Delta w_{a1i}}{\Delta w_{e1i} - \Delta w_{n1i}}, \tag{20b}$$

$$C_{3i} = \frac{\Delta w_{a2i}}{\Delta w_{e2i} - \Delta w_{n2i}}, \tag{20c}$$

$$C_{4i} = \frac{\Delta w_{a3i}}{\Delta w_{e3i} - \Delta w_{n3i}}, \tag{20d}$$

where ΔP_{ni} is the translational deflection vectors in x, y and z directions and Δw_{1ni}, Δw_{2ni} and Δw_{3ni} are orientation deflections for no-load conditions, respectively. The load coefficient, as to the accuracy of the motion constraint in the ith point of the path, can be determined as:

$$C_{i-\text{Accuracy}} = \min\{C_{1i}, C_{2i}, C_{3i}, C_{4i}\}. \tag{21}$$

And the load coefficient, as to the accuracy of the motion constraint ($C_{\text{Load}-\text{Accuracy}}$) for the whole path, can be selected as the minimum value of $C_{i-\text{Accuracy}}$.

Determination of Maximum Dynamic Load for a Given Trajectory

After determining the load coefficient of the actuator constraint ($C_{\text{Load}-\text{Torque}}$) and the load coefficient of the accuracy constraint ($C_{\text{Load}-\text{Accuracy}}$), the load coefficient of the whole of the given trajectory can be determined as the minimum value between $C_{\text{Load}-\text{Torque}}$ and $C_{\text{Load}-\text{Accuracy}}$. Then, the maximum dynamic load for a given trajectory can be determined as follows:

$$m_L = C_{\text{Load}} m_e. \tag{22}$$

COMPUTATIONAL PROCEDURE FOR DETERMINING DYNAMIC LOAD CARRYING CAPACITY

By imposing the joint actuator torque capacity and the accuracy of motion constraints, a computational procedure for determining the DLCC of a 6UPS-Stewart platform, is outlined and also flow-charted in Figures 3a and 3b. In order to calculate the load coefficient of a given path, first, the actuator forces under no-load and sample load conditions are determined and, then, the load coefficient, due to the actuator torque capacity constraint ($C_{i-\text{Torque}}$) and the load coefficient, due to the accuracy of motion constraint ($C_{i-\text{Accuracy}}$), are determined, for each point of the path. Then, the load coefficient of the current point of path ($C_{i-\text{Load}}$) is considered as the minimum value of them. The load coefficient of the whole of the path is considered as the minimum value of C_{Load}.

SIMULATION RESULTS AND DISCUSSIONS

Based on the above algorithm, a computer program was developed to solve the inverse dynamics and compute the maximum DLCC of the 6UPS-Stewart platform (shown in Figure 4) for a given trajectory, using Mathematica software. Figure 4 shows the location of the universal and ball joints and the initial location of the moving platform. In this procedure, first, it is assumed that the manipulator is a rigid joint and the maximum load of the given trajectory is determined by imposing the actuator force capacity as the limiting factor. Then, it is assumed that the prismatic joints of the manipulator are flexible and the maximum load of the given trajectory is determined by imposing the accuracy of motion as the limiting factor.

The system of equations is derived and expanded by using a numerical value for its parameters in Table 1. The following system of equations can be solved to find actuator forces:

$$\begin{pmatrix} J_{p11} & \cdots & J_{p16} \\ \vdots & \ddots & \vdots \\ J_{p61} & \cdots & J_{p66} \end{pmatrix}^T \begin{pmatrix} \tau_1 \\ \vdots \\ \tau_6 \end{pmatrix} + \begin{pmatrix} F_{p1} \\ \vdots \\ F_{p6} \end{pmatrix} + \sum_{i=1}^{6} \left(\begin{pmatrix} J_{1iAi11} & \cdots & J_{1iAi16} \\ \vdots & \ddots & \vdots \\ J_{1iAi61} & \cdots & J_{1iAi66} \end{pmatrix}^T \begin{pmatrix} F_{1iAi1} \\ \vdots \\ F_{1iAi6} \end{pmatrix} + \begin{pmatrix} J_{2iAi11} & \cdots & J_{2iAi16} \\ \vdots & \ddots & \vdots \\ J_{2iAi61} & \cdots & J_{2iAi66} \end{pmatrix}^T \begin{pmatrix} F_{2iAi1} \\ \vdots \\ F_{2iAi6} \end{pmatrix} \right) = 0, \tag{23}$$

where details of J_p, J_{1Aii}, J_{2Aii}, F_{1Aii} and F_{2Aii} can be found in Appendix. The deflection vector of the end-effector at each point of the path is determined by:

$$\begin{bmatrix} \Delta w_1 \\ \Delta w_2 \\ \vdots \\ \Delta w_6 \end{bmatrix} = \begin{bmatrix} J_{p11} & J_{p12} & \cdots & J_{p16} \\ J_{p21} & J_{p22} & \cdots & J_{p26} \\ \vdots & \vdots & \ddots & \vdots \\ J_{p61} & J_{p62} & \cdots & J_{p66} \end{bmatrix} \cdot \begin{bmatrix} \frac{1}{K_1} & 0 & 0 & 0 \\ 0 & \frac{1}{K_1} & 0 & 0 \\ \vdots & \vdots & \ddots & \vdots \\ 0 & 0 & 0 & \frac{1}{K_1} \end{bmatrix} \cdot \begin{bmatrix} F_{a1} \\ F_{a2} \\ \vdots \\ F_{a6} \end{bmatrix}. \tag{24}$$

Simulation Results

Various desired trajectories were simulated and a simple one was solved to illustrate the algorithm. In

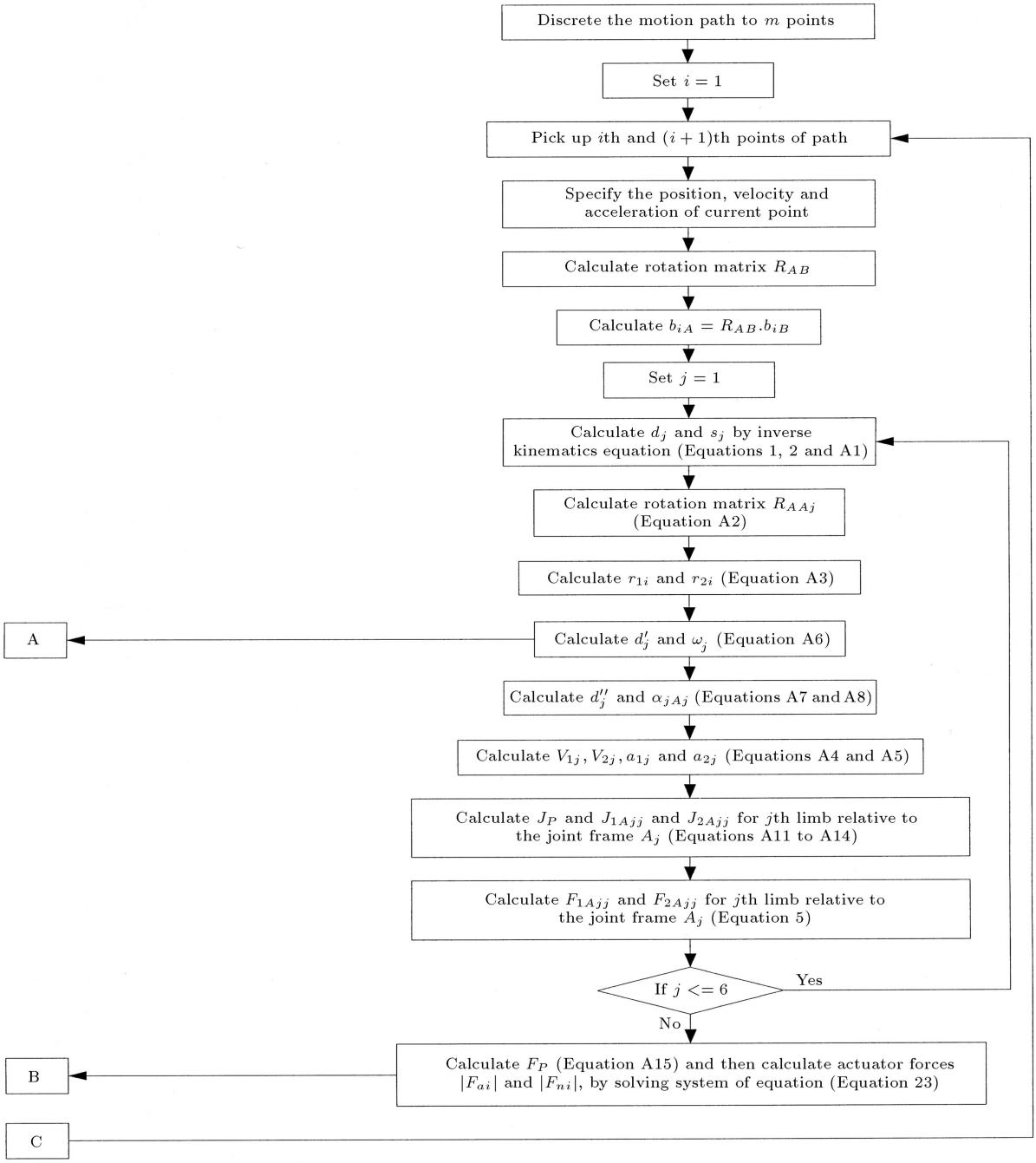

Figure 3a. Computational flowchart for kinematics and dynamic analyis of the mnaipulator.

this example, it is assumed that the platform starts at rest and accelerates with a constant acceleration of $a = [-0.15, -0.20, -0.30]$ m/s^2 for a period of 1 second, while all the other parameters are held constant. Furthermore, the initial conditions for the position and orientation of the moving platform origin are $P_1 = \{0, 0, 0.41143, 0, 0, 0\}$ and its velocity and acceleration are zero. The velocity and acceleration of the trajectory are obtained by differentiating the trajectory by a sampling time of 0.01 seconds. The displacement, velocity, acceleration and force of the actuators are determined by using the kinematic and dynamic models of the manipulators for a given trajectory, as shown in Figures 5a to 5d.

For a given hydraulic actuator system and the mass of a platform of 8.633 kg, by considering only the actuator torque capacity constraint, the maximum load that can be carried in a given path is 1022.38 kg, which the given actuators can carry in executing the trajectory. Figure 6 shows the time-varying forces

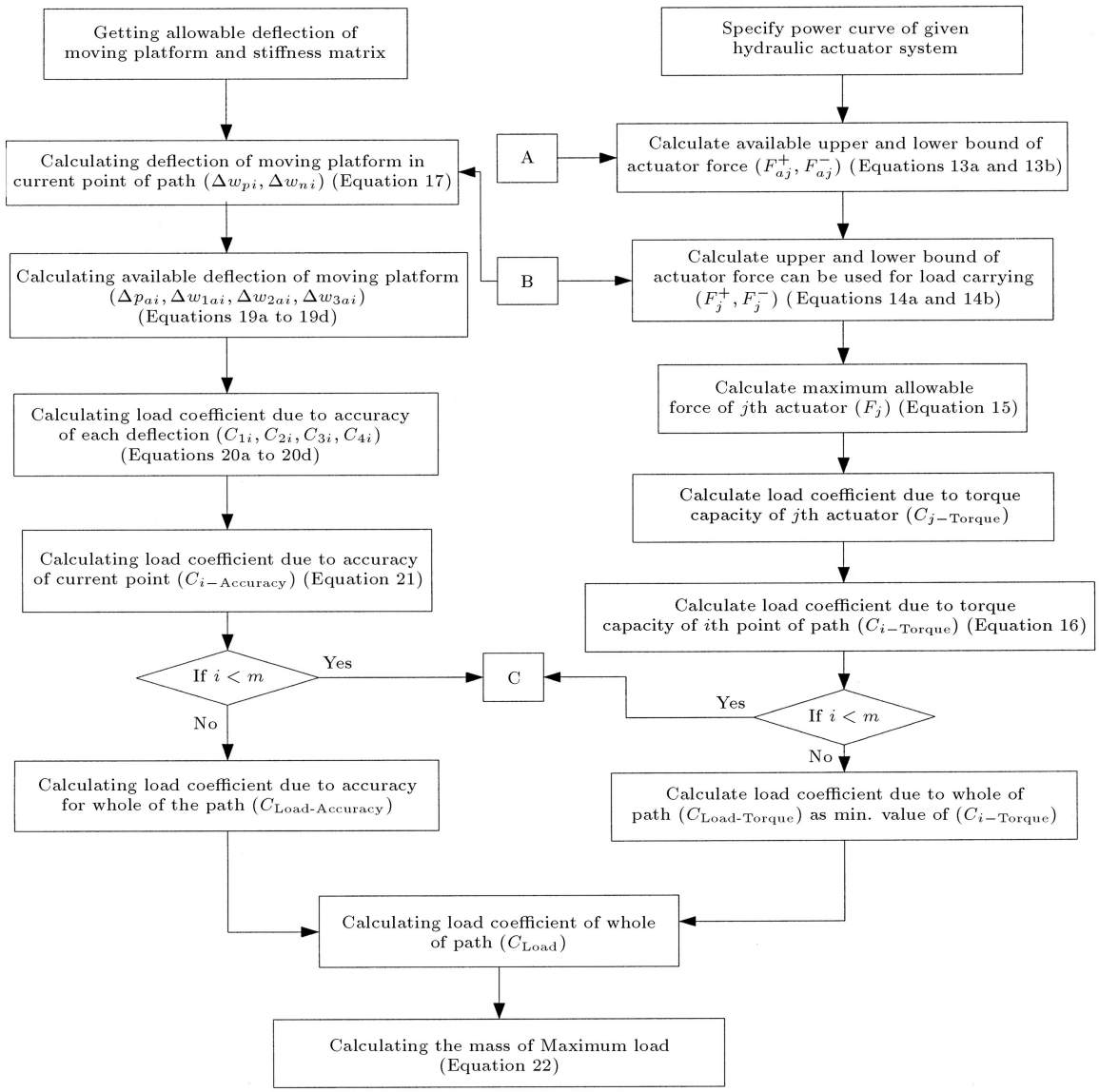

Figure 3b. Computational flowchart for DLCC determination of the manipulator.

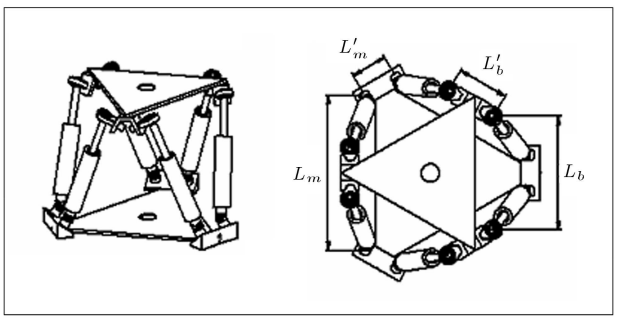

Figure 4. 6UPS-Stewart platform.

required to execute the trajectory against the upper and lower bounds of the available forces, which depend on the joint velocity.

It is seen that the load so determined uses joints 1 and 2 to their maximum extent at about 0.5 seconds, while other joints bounds are not reached during the course. By considering the prismatic joints flexibility, when the actual trajectory of the moving platform is plotted in based coordinates, with the prescribed upper and lower bounds of $\delta^P = 0.0052$ m and $\delta_1^r = \delta_2^r = \delta_3^r = 0.01$ deg, as shown in Figures 7a to 7c, it is apparent that the desired tracking accuracy cannot be achieved for $m_{\text{Load}} = 1022.38$ kg (out of accuracy zones of the moving platform are shown in Figures 7a to 7c for a given trajectory). This clearly demonstrates the need to impose an additional constraint on end-effector deflection when the DLCC is determined for a flexible manipulator.

By imposing the actuator torque capacity and motion accuracy constraints on DLCC determination of the manipulator, a load of $m_{\text{Load}} = 803.465$ kg was found as the maximum payload. It means that

Table 1. Numerical value for simulation.

Manipulator Parameters		
Parameter	**Value**	**Unit**
L_b, L'_b	386.75, 100.00	mm
L_m, L'_m	290.55, 140.82	mm
$\{I_{pcxx}, I_{pcyy}, I_{pczz}\}$	{107220.53,107220.53,210552.33}	kg.mm^2
e_1, e_2	115.46, 87.46	mm
m_P, m_1, m_2	8.633, 0.832, 0.669	kg
$\{I_1cxx, I_1cyy, I_1czz\}$	{4802.25,388.51,4802.25}	kg.mm^2
$\{I_2cxx, I_2cyy, I_2czz\}$	{3692.99,57.92,3692,99}	kg.mm^2
C_P	{0,0,9.35}	mm
Hydraulic Actuator System Parameters		
A_1, A_2	201.06, 102.52	mm^2
P_S	10.3	MPa
L, w, u	200, 34, 20	mm
β	1.03	GPa
C_1, C_2, C_3, C_4	0.65	-
ρ	872	kg/m^{-3}

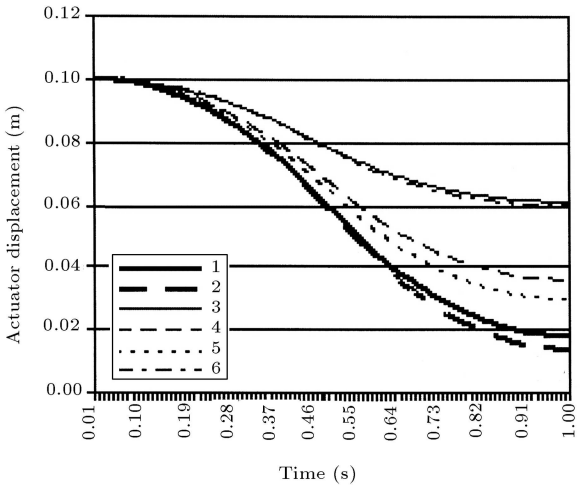

Figure 5a. Joint displacement.

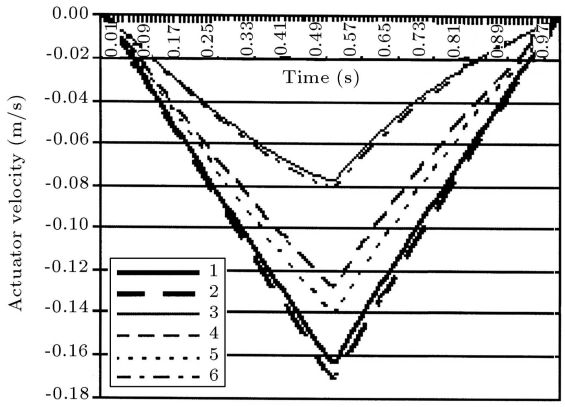

Figure 5b. Joint velocity.

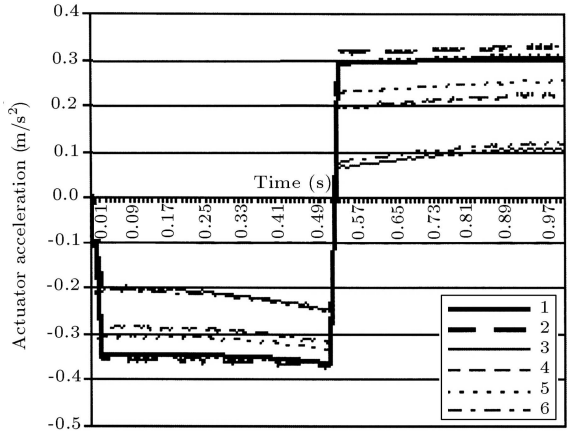

Figure 5c. Joint acceleration.

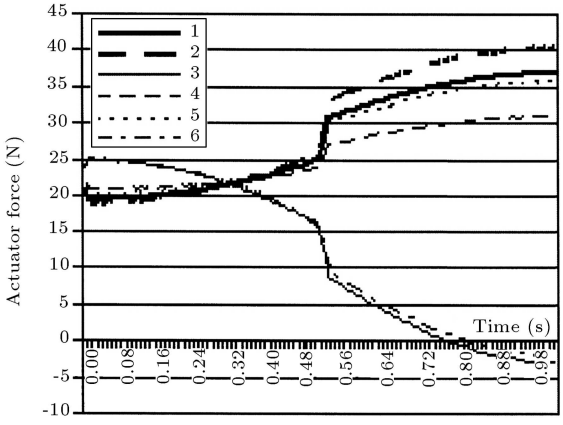

Figure 5d. Force of actuators (no load condition).

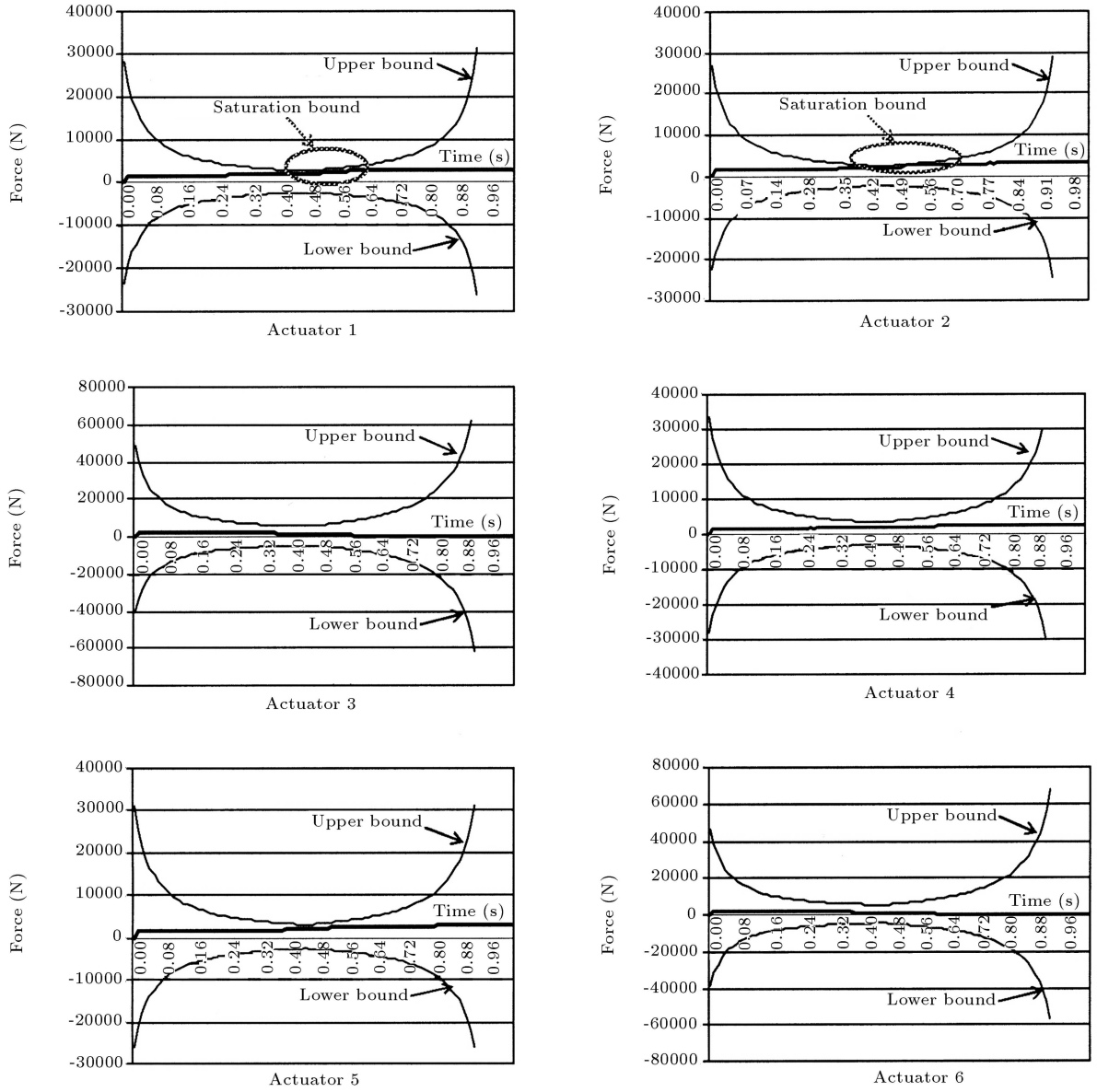

Figure 6. Force of joint actuated in maximum load carrying.

neither of the constraints is violated in executing the same trajectory and end-effector deflection requirements when the manipulator carries the calculated maximum payload. By imposing the actuator torque capacity and motion accuracy constraints, the desired and actual trajectory against deflection bounds is shown in Figures 8a to 8f for the same trajectory and end-effector deflection requirements.

As shown in Figures 8a to 8f, the parts of the path which were out of alignment under the first constraint, did coincide on the bound of the path.

CONCLUSION

The main objective of this investigation is to formulate DLCC and to determine the maximum load for a typical parallel manipulator, based on the Stewart mechanism and imposing actuator torque capacity and accuracy of motion constraints. Simulation results of an introduced typical 6UPS-Stewart platform show an acceptable operation of model and algorithm. The simulation results of several typical paths show that, when the first constraint is imposed, the maximum load is about 20% more than when both constraints are imposed. In the other words, the simulation result shows that, if only the first constraint is imposed for flexible joint manipulators, the load so determined may result in substantial deflections at the end-effector when it moves through the predefined dynamic trajectory. In order to be able to control the end-effector tracking precision, addition of the second constraint is necessary.

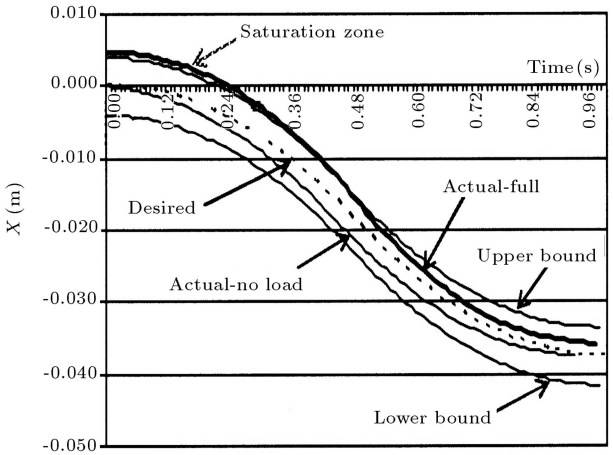

Figure 7a. X direction of desired and actual trajectory against deflection bound without accuracy constraint.

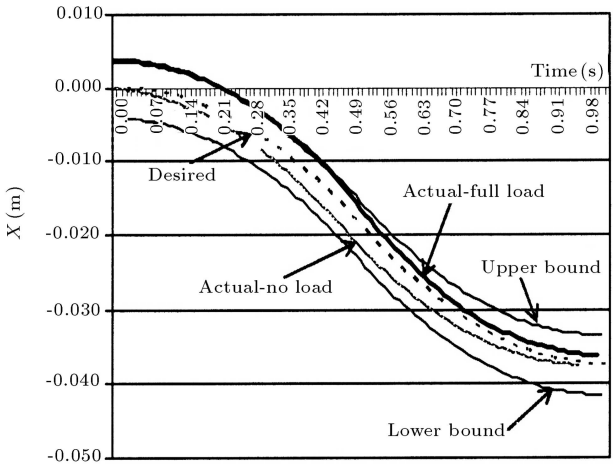

Figure 8a. X direction of desired and actual trajectory against deflection bound with accuracy constraint.

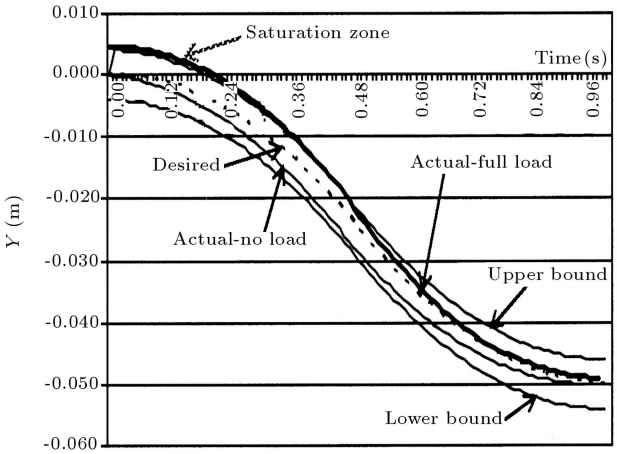

Figure 7b. Y direction of desired and actual trajectory against deflection bound without accuracy constraint.

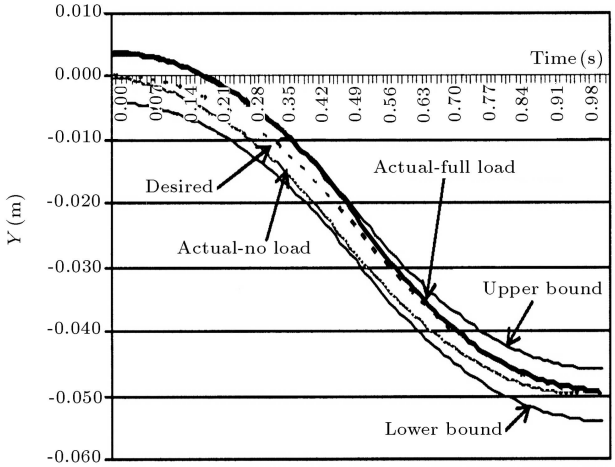

Figure 8b. Y direction of desired and actual trajectory against deflection bound with accuracy constraint.

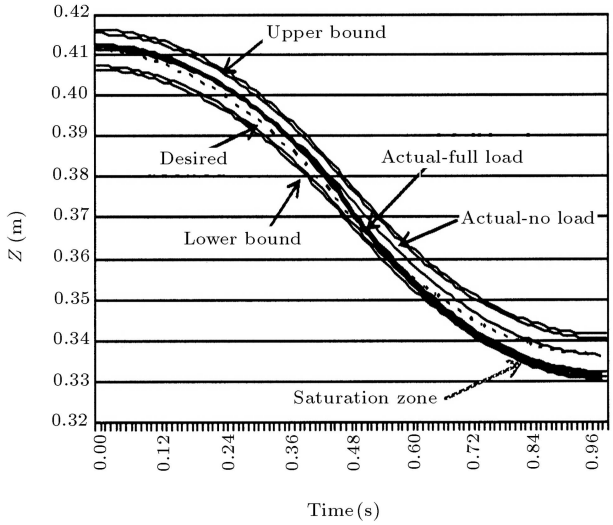

Figure 7c. Z direction of desired and actual trajectory against deflection bound without accuracy constraint.

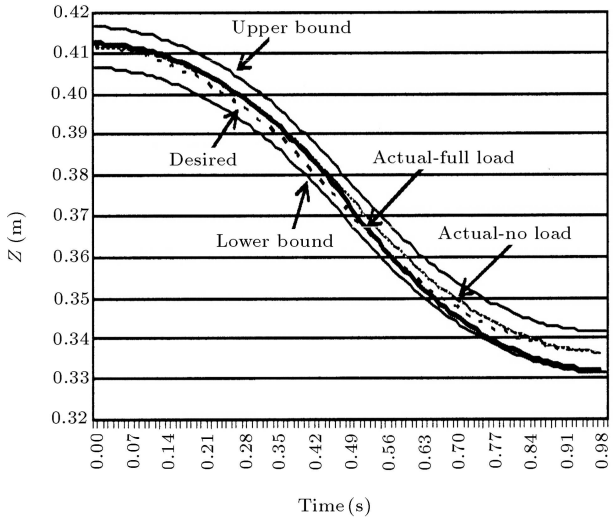

Figure 8c. Z direction of desired and actual trajectory against deflection bound with accuracy constraint.

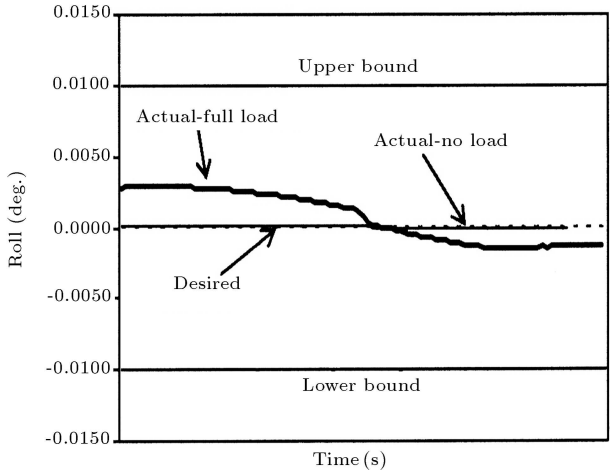

Figure 8d. φ rotation of desired and actual trajectory against deflection bound with accuracy constraint.

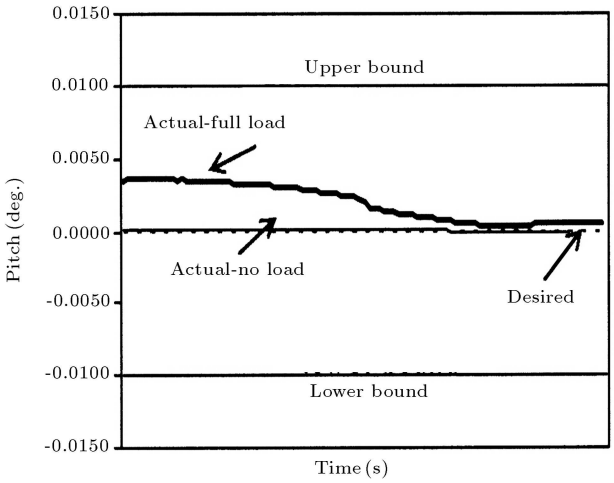

Figure 8e. θ rotation of desired and actual trajectory against deflection bound with accuracy constraint.

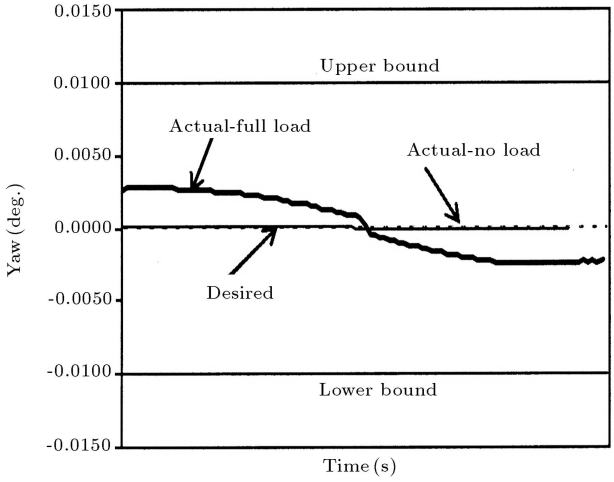

Figure 8f. ψ rotation of desired and actual trajectory against deflection bound with accuracy constraint.

REFERENCES

1. Shokri, M. "Kinematics and dynamics modeling of closed loop manipulators based on Stewart mechanism and DLCC analysis of a 6UPS-Stewart platform", MSc Thesis, Department of Mech. Eng., Iran University of Science and Technology, Tehran, I.R. Iran (2005).
2. Korayem, M.H. and Shokri, M. "Maximum dynamic payload carrying capacity of 6UPS-Stewart platform manipulator", *Tehran International Congress on Manufacturing Engineering (TICME2005)*, December 12-15, Tehran, Iran (2005).
3. Wang, L.T. and Ravani, B. "Dynamic load carrying capacity of mechanical manipulators- Part I: Problem formulation", *Trans. ASME J. Dynamic Systems, Meas. Control*, **110**, pp 46-52 (1988).
4. Wang, L.T. and Ravani, B. "Dynamic load carrying capacity of mechanical manipulators-Part II: Computational procedure and applications", *Trans. ASME J. Dynamic Systems, Meas., Control*, **110**, pp 53-61 (1988).
5. Bowling, A. and Khatib, O. "Dynamic load criteria in actuator selection for desired dynamic performance", *Advanced Robotics*, **17**(7), pp 641-656 (2003).
6. Bowling, A. and Khatib, O. "The dynamic capability equations: A new tool for analyzing robotic manipulator performance", *IEEE Transaction on Robotics and Automation*, **21**(1), pp 526-531 (2005).
7. Wang, C.E., Timoszyk, W.K. and Bobrow, J.E., *Payload Maximization for Open Chained Manipulators: Finding Weightlifting Motions for a Puma 762 Robot*, Department of Mech. and Aerospace Engineering University of California, Irvine, CA, USA (2000).
8. Korayem, M.H. and Basu, A. "Dynamic load carrying capacity of robotic manipulators with joint elasticity imposing accuracy constraints", *Robotics and Autonomous Systems*, **13**, pp 219-229 (1994).
9. Kim, H.S. and Choi, Y.J. "Forward/inverse force transmission capability analyses of fully parallel manipulators", *IEEE Transactions on Robotics and Automation*, **17**(4), pp 526-531 (2001).
10. Zhao, Y.S., Lu, L., Ahao, T.S., Du, Y.H. and Huang, Z. "The novel approaches for computing the dynamic load-carrying capacity of multiple cooperating robotic manipulators", *Mechanism and Machine Theory*, **34**, pp 637-643 (1998).
11. Yue, S., Tso, S.K. and Xu, W.L. "Maximum-dynamic-payload trajectory for flexible robot manipulators with kinematic redundancy", *Mechanism and Machine Theory*, **36**, pp 785-800 (2001).
12. Merlet, J.-P. "Efficient estimation of the external articular forces of a parallel manipulator in a translation workspace", *IEEE International Conference on Robotics and Automation*, Belgium (1998).
13. Nokleby, S.B., Fisher, R., Podhorodeski, R.P. and Firmani, F. "Force capabilities of redundantly-actuated parallel manipulators", *Mechanism and Machine Theory*, **40**(5), pp 578-599 (2004).

14. Sirouspour, M.R. and Salcudeam, S.E. "A new approach to the control of a hydraulic Stewart platform", *Lecture Notes in Control and Information Science*, **271**, Experimental Robotics VII ISER, pp 447-460 (2006).

APPENDIX

$$d_i = \pm[P^T P + b_{iB}^T b_{iB} + a_i^T a_i + 2P^T[R_{AB} b_{iB}] - 2P^T a_i - 2[R_{AB} b_{iB}]^T a_i]^{\frac{1}{2}}, \tag{A1}$$

$$R_{AiA} = \begin{bmatrix} \cos\theta_i . \sin\phi_i & \cos\phi_i & \sin\theta_i . \sin\phi_i \\ -\sin\theta_i & 0 & \cos\theta_i \end{bmatrix}, \tag{A2}$$

$$r_{1i} = a_i + e_1 s_{iA}, \qquad r_{2i} = a_i + (d_i - e_2) s_{iA}, \tag{A3}$$

$$v_{1iAi} = e_1(\omega_{iAi} \times s_{iAi}),$$

$$v_{2iAi} = (d_i - e_2)(\omega_{iAi} \times s_{iAi}) + \dot{d}_i s_{iAi}, \tag{A4}$$

$$a_{1iAi} = e_1(\dot{\omega}_{iAi} \times s_{iAi}) + e_1 \omega_{iAi} \times (\omega_{iAi} \times s_{iAi}),$$

$$a_{2iAi} = (d_i - e_2)(\dot{\omega}_{iAi} \times s_{iAi}) + (d_i - e_2)\omega_{iAi} \times (\omega_{iAi} \times s_{iAi}) + \ddot{d}_i s_{iAi} + 2\dot{d}_i(\omega_{iAi} \times s_{iAi}), \tag{A5}$$

$$\omega_i = s_i \times \frac{\dot{S}_i}{d_i}, \qquad \dot{d}_i = s_i . \dot{S}_i, \tag{A6}$$

$$\ddot{d}_i = s_i . a_p + s_i . (\omega_p \times (\omega_p \times b_{iA})) + \frac{1}{d_i}(\dot{S}_i - \dot{d}_i s_i)^2, \tag{A7}$$

$$\alpha_i = \frac{1}{d_i}(s_i \times a_p) + \frac{1}{d_i}(s_i \times (\omega_p \times (\omega_p \times b_{iA})) - 2\dot{d}_i \omega_p), \tag{A8}$$

$$I_{1iAi} = I_{1ic} + m_{1i} e_1^2 \mathrm{diag}(1,1,0),$$

$$I_{2iAi} = I_{2ic} + m_{2i}(d_i - e_2)^2 \mathrm{diag}(1,1,0), \tag{A9}$$

$$I_p = R_{AB} I_{pc} R_{AB}^T, \tag{A10}$$

$$v_{bi} = v_p + \omega_p \times b_{iA}, \tag{A11}$$

$$J_{bi} = \begin{pmatrix} 1 & 0 & 0 & 0 & b_{iz} & -b_{iy} \\ 0 & 1 & 0 & -b_{iz} & 0 & b_{ix} \\ 0 & 0 & 1 & b_{iy} & -b_{ix} & 0 \end{pmatrix}, \tag{A12}$$

$$v_{biAi} = J_{biAi} \dot{x}_p = \begin{pmatrix} J_{biAix} \\ J_{biAiy} \\ J_{biAiz} \end{pmatrix} \dot{x}_p, \tag{A13}$$

$$J_p = \begin{pmatrix} J_{b1A1z} \\ J_{b2A2z} \\ \vdots \\ J_{b6A6z} \end{pmatrix}, \qquad J_{1iAi} = \frac{1}{d_i} \begin{pmatrix} e_1 J_{biAix} \\ e_1 J_{biAiy} \\ 0_{1\times 6} \\ -J_{biAiy} \\ J_{biAix} \\ 0_{1\times 6} \end{pmatrix},$$

$$J_{2iAi} = \frac{1}{d_i} \begin{pmatrix} (d_i - e_2) J_{biAix} \\ (d_i - e_2) J_{biAiy} \\ d_i J_{biAiz} \\ -J_{biAiy} \\ J_{biAix} \\ 0_{1\times 6} \end{pmatrix}, \tag{A14}$$

$$F_p = \begin{bmatrix} f_p \\ n_p \end{bmatrix} = \begin{bmatrix} m_p g - m_p a_p \\ -I_p \alpha_p - \omega_p \times (I_p \omega_p) \end{bmatrix}. \tag{A15}$$